

LA-UR- 08-6754

Approved for public release;
distribution is unlimited.

Title: Rediscovering Signal Complexity as a Teleseismic Discriminant (U)

Author(s): Dale N. Anderson, EES-17

Steven R Taylor, EES-17

Intended for: Pure and Applied Geophysics



Los Alamos National Laboratory, an affirmative action/equal opportunity employer, is operated by the Los Alamos National Security, LLC for the National Nuclear Security Administration of the U.S. Department of Energy under contract DE-AC52-06NA25396. By acceptance of this article, the publisher recognizes that the U.S. Government retains a nonexclusive, royalty-free license to publish or reproduce the published form of this contribution, or to allow others to do so, for U.S. Government purposes. Los Alamos National Laboratory requests that the publisher identify this article as work performed under the auspices of the U.S. Department of Energy. Los Alamos National Laboratory strongly supports academic freedom and a researcher's right to publish; as an institution, however, the Laboratory does not endorse the viewpoint of a publication or guarantee its technical correctness.

Rediscovering Signal Complexity as a Teleseismic Discriminant

Short title: Teleseismic Signal Complexity

Steven R. Taylor
Rocky Mountain Geophysics
167 Piedra Loop
Los Alamos, NM 87544
USA
srt-rmg@comcast.net
Fax: 505-672-3344

Dale N. Anderson^{*}
Pacific Northwest National Laboratory
PO Box 999
Richland, WA 99352
USA

October 14, 2008

^{*} Now at

Los Alamos National Laboratory
PO Box 1663; MS F665
Los Alamos, NM 87545

Submitted to Pure and Applied Geophysics

RMG-006-2008

Keywords: Complexity, teleseismic, discriminant

Abstract

We re-examine the utility of teleseismic seismic complexity discriminants in a multivariate setting using United Kingdom array data. We measure a complexity discriminant taken on array beams by simply taking the logarithm of the ratio of the P wave coda signal to that of the first arriving direct P wave (β_{CF}). The single station complexity discriminant shows marginal performance with shallow earthquakes having more complex signatures than those from explosions or deep earthquakes. Inclusion of secondary phases in the coda window can also degrade performance. However, performance improves markedly when two-station complexity discriminants are formed showing false alarm rates similar to those observed for network $m_b - M_s$. This suggests that multistation complexity discriminants may ameliorate some of the problems associated with $m_b - M_s$ discrimination at lower magnitudes. Additionally, when complexity discriminants are combined with $m_b - M_s$ there is a tendency for explosions, shallow earthquakes and deep earthquakes to form three distinct populations. Thus, complexity discriminants may follow a logic that is similar to $m_b - M_s$ in terms of the separation of shallow earthquakes from nuclear explosions, although the underlying physics of the two discriminants is significantly different.

Introduction

Seismic complexity measurements have been investigated for quite some time with marginal results (e.g. Arora and Basu, 1984), but recent work suggests that complexity measures may be effective for multivariate teleseismic event screening and regional discrimination (Koch and Schlittenhardt, 2002; Ortiz *et al.*, 2002). Many studies of seismic signal complexity focused on examining the physical mechanisms behind simple and complex waveforms (e.g. Douglas *et al.*, 1973; 1974; Barley, 1977; Bowers, 1996). Typically shallow earthquakes present complex P wave signatures relative to single-charge explosions. This is mainly due to the fact that earthquakes can generate complex signals from the rupture process including reflected depth phases such as pP and sP . Simulations of Bowers (1996) indicated that multistation complexity measurements would reduce false alarm rates. The reasoning is that at certain azimuths and low signal-to-noise ratio, only P, pP or sP may be observed from an earthquake resulting in an apparent simple waveform. Multistation complexity measures at different azimuths will mitigate this effect thereby reducing false alarm rates and allowing inclusion of stations having higher signal-to-noise ratio. In contrast, pure explosions are generated by simple, impulsive point sources.

Exceptions to this are earthquakes producing simple P waveforms such as those with shallow dip-slip mechanisms, signals along azimuths having two of P , pP , and sP radiation nodes, and deep earthquakes. Explosions may also have complex P waves generated by secondary sources such as tectonic release or spall (e.g. Wallace *et al.*, 1983; Wallace, 1991). But, it is generally accepted that these sources contribute mainly to later arriving shear waves and do not significantly affect the P waves except for possibly very large explosions. Thus, seismic measures of complexity cannot be used to positively identify an explosion without some indication of depth, but may be used to rule out most shallow earthquakes and therefore may add another piece to the multivariate source classification puzzle. Complexity discriminants may follow a logic that is similar to $m_b - M_s$ in terms of separation of shallow earthquakes from nuclear explosions, although the physics of the two discriminants are significantly different.

To date, the teleseismic Event Classification Matrix (ECM) of Anderson *et al.*, (2007) has examined four discriminants: Depth from P-wave arrival times, depth from P-wave surface reflections, m_b versus M_s , and polarity of the first motion. The Complexity Factor (CF) discriminant has not yet been examined for inclusion into the ECM. The purpose of our work is to examine the efficacy of a complexity discriminant particularly in tandem with other teleseismic discriminants such as the m_b versus M_s .

Data

We have acquired a large data set consisting of 709 worldwide earthquakes and explosions recorded at the four United Kingdom (UK) arrays kindly provided by the Blacknest Seismological Centre (e.g. Taylor and Marshall, 1991). We have selected a subset of 116 nuclear explosions, 29 shallow earthquakes (ISC reported depth < 50 km) and 12 deep earthquakes (ISC reported depth > 50 km; **Figure 1**). Body wave magnitudes for this study ranged from 4.80 to 6.96 and distances from 16.3 to 176.1 degrees.

***** Insert Figure 1 here *****

We have computed and analyzed non-optimal beams for 2318 station and event pairs. For each station and event pair we have made a P-wave arrival time pick as well as a polarity estimate. We have also computed a complexity factor (β_{CF}) given by

$$\beta_{CF} = \log(E_c/E_s) \quad (1)$$

where E_c is the average energy (mean square) of the coda in the 5 to 25 second window after the P arrival time, E_s is the average signal energy in the 5 second window after the P arrival time. We also compute the average noise energy in the 20 seconds preceding the P arrival time for signal-to-noise testing. For our preliminary analysis we are using a 0.25 to 4 Hz band for all measurements taken on the non-optimal beam. In **Figures 2, 3 and 4** we show examples of a Chinese nuclear explosion, a shallow earthquake (29 km) in Iran and a deep earthquake (97 km) beneath Chile.

***** Insert Figures 2, 3 and 4 here *****

Both the nuclear explosion and deep earthquake recordings are characterized by relatively simple waveforms and negative β_{CF} values. One exception is for the Lop Nor explosion recorded at the GBA array in India. GBA is located at approximately 30° from Lop Nor and the coda often is contaminated by caustics associated with upper mantle triplications. This probably resulted in the disappointing complexity discriminant results of Arora and Basu (1984) who analyzed Lop Nor explosions at GBA. As will be shown below, other examples of upper mantle triplications increasing the value of complexity measurements are observed at YKA for NTS explosions. These observations suggest that teleseismic P-wave complexity measurements taken at upper mantle triplication distances may have complexity factors that are biased high using the existing window definitions. However, on the whole, our work suggests that the highest complexity factors are not necessarily always observed at upper mantle triplication distances. The issue of upper-mantle triplications can be ameliorated with data quality restrictions on distance ranges used for constructing the complexity discriminant or by forming multistation complexity discriminants as discussed below.

Complexity factors (β_{CF}) are shown in **Figure 5** as a function of m_b and in **Figure 6** as a function of distance for each of the array stations. We have selected earthquakes (occurring in 1980) from our dataset that have m_b and M_s values obtained from the International Seismic Centre and explosions having m_b and M_s from Stevens and Murphy (2001). For

the dataset we have processed there are very few explosion M_s measurements from the ISC that is why we supplemented them with those of Stevens and Murphy (2001). Although the M_s values and some of the m_b values are from different catalogs and sources, our main point here is to illustrate the synergy obtained by combining $m_b - M_s$ and β_{CF} . Following Anderson *et al.*, (2007) we have partitioned the events into nuclear explosions (EX), shallow earthquakes (SEQ; depth < 50 km) and deep earthquakes (DEQ; depth > 50 km). Although β_{CF} shows quite a bit of scatter, there is a notable stratification of the event types with nuclear explosions having the lowest complexity factors, deep earthquakes having intermediate complexity factors and shallow earthquakes having the highest complexity factors. There does appear to be a strong dependence of β_{CF} with m_b or distance.

***** Insert Figures 5 and 6 here *****

Interestingly, the stratification showing increased complexity from nuclear explosions to deep earthquakes to shallow earthquakes is similar to patterns observed for the m_b versus M_s discriminant. Of course, the underlying physics between the two discriminants is significantly different. Below we investigate the relationship between signal complexity and the $m_b - M_s$ discriminant in a bivariate setting. Although the two discriminants may be correlated as a function of source type, we suspect that the residuals after accounting for correlation may be independent resulting in increased identification power when combined. Many statistical classification theories are readily available to analyze correlated discriminants.

Figure 7 shows $m_b - M_s$ as a function of m_b for the events that we have β_{CF} measurements. For this particular dataset there is complete separation between earthquakes and explosions. Although there is a tendency for the deep earthquakes to have a higher $m_b - M_s$ than shallow earthquakes, there is quite a bit of intermingling between the shallow and deep earthquakes.

***** Insert Figure 7 here *****

Figure 8 is a bivariate plot of $m_b - M_s$ versus complexity (β_{CF}) at the four UK array stations. At each array station there is complete separation of earthquakes and explosions and a tendency for signal complexity to increase as $m_b - M_s$ decreases. Most notably, the

DEQ and SEQ populations are showing signs of separation as well. This has the important implication that signal complexity can be effectively combined with other teleseismic discriminants in the multivariate ECM framework of Anderson *et al.*, (2007).

***** Insert Figure 8 here *****

Simulations of Bowers (1996) indicated that multistation complexity measurements would reduce false alarm rates. The reasoning is that at certain azimuths and low signal-to-noise ratio, only P , pP or sP may be observed from an earthquake resulting in an apparent simple waveform. However, multistation measures at different azimuths will mitigate this effect thereby reducing false alarm rates. To test this, we formed bivariate plots of β_{CF} for each combination of UK array stations (Figure 9). As predicted by Bowers (1996) we observe significantly improved separation between earthquakes and explosions relative to those observed from a single array (Figure 5).

***** Insert Figure 9 here *****

To quantify the observations, we computed false alarm rates for each array pair shown in Figure 9 using a leave-one-out procedure. To do this we computed the linear discrimination function, $G(\mathbf{v})$, for explosions (X) and shallow earthquakes (Q) given by

$$G(\mathbf{v}) = \mathbf{v}^T \Sigma^{-1} (\mu_Q - \mu_X) - \frac{1}{2} (\mu_Q + \mu_X)^T \Sigma^{-1} (\mu_Q - \mu_X) + \ln \frac{P(Q)}{P(X)} \quad (2)$$

where \mathbf{v} is a vector of observations, μ_Q and μ_X are mean vectors for the shallow earthquake and explosion populations, respectively (Hand, 1981; Taylor 1996). We assume equal covariance matrices for earthquakes and explosions, Σ , and $P(Q)$ and $P(X)$ are prior probabilities of occurrence. We included only shallow earthquakes in this analysis in order to compare identification performance metrics with those of Fisk *et al.*, (2002) which already had a depth screening criteria included. Similarly, the ECM formulation of Anderson *et al.*, (2007) already includes two independent measures of depth.

The discrimination functions for each UK array pair, $G(\mathbf{v})$, are shown in **Figure 10**. Using leave-one-out cross validation, we estimated false alarm error rates, $P(X|Q)$, where we have assumed a prior probability of occurrence, $P(X) = 0.85$ in order to misidentify very few explosions. The false alarm rates range from 0.06 to 0.33 with an average value of 0.21. These two station complexity false alarm rates are similar to those observed by Fisk *et al.*, (2002) for network-average $M_s:m_b$ at the prototype International Data Center. Figure 10 is another illustration suggesting that complexity factor appears to have a negative correlation with $m_b - M_s$ as observed in Figure 8. In other words, events within a given population having a high complexity factor tend to have a lower $m_b - M_s$.

Conclusions

We have re-examined teleseismic signal complexity as a means of improving overall discrimination capability in a multivariate framework. Although the complexity discriminant by itself shows marginal performance, we have indications that it can be effectively combined other discriminants such as $m_b - M_s$ to improve teleseismic identification in the ECM framework of Anderson *et al.*, (2007). When complexity discriminants are combined with $m_b - M_s$ there is a tendency for explosions, shallow earthquakes and deep earthquakes to form three distinct populations. Importantly, multistation complexity discriminants may perform as well as network $m_b - M_s$. Clearly, further work is needed to examine the efficacy of teleseismic complexity at smaller magnitudes and to examine regional complexity discriminants as in Ortiz *et al.*, (2002).

Acknowledgments

We gratefully acknowledge the advice and assistance provided by John Young, David Bowers and Neil Selby of the Blacknest Seismological Centre for the release of the important UK array historic dataset. We also thank Jeff Stevens for kindly providing the tables contained in Stevens and Murphy (2001). The insightful comments of two anonymous reviewers are also appreciated. This work was completed under the auspices of the U.S. Department of Energy by Pacific Northwest National Laboratory under contract DE-AC05-RLO1830.

References

- Anderson, D.N. and S.R. Taylor (2002), Application of Regularized Discrimination Analysis to regional seismic event identification, *Bull. Seism. Soc. Am.*, 92, 2391-2399.

- Anderson, D.N., D.K. Carlson, M.A. Tinker, G.D. Kraft and K.D. Hutchenson (2007), A mathematical statistics formulation of the teleseismic explosion identification problem with multiple discriminants, *Bull. Seism. Soc. Am.*, 97, 1730-1741.
- Arora, S.K. and T.K Basu (1984), A source discrimination study of a Chinese seismic event of May 4, 1983, *Tectonophysics*, 109, 241-251.
- Barley, B.J., The origin of complexity in some P seismograms from deep earthquakes (1977), *Geophys. J. R. Astr. Soc.*, 49, 773-777.
- Bowers, D. (1996), On the probability of mistaking an earthquake for an explosion using the simplicity of P, *Bull. Seism. Soc. Am.*, 86, 1925-1934.
- Douglas, A., P.D. Marshall, P.G. Gibbs, J.B. Young and C. Blamey (1973), P signal complexity re-examined, *Geophys. J. R. Astr. Soc.*, 33, 195-221.
- Douglas, A., J.B. Young and J.A. Hudson (1974), Complex P-wave seismograms from simple earthquake sources, *Geophys. J. R. astr. Soc.*, 37, 141-150.
- Fisk, M.D., D. Jepsen and J.R. Murphy (2002), Experimental seismic event-screening criteria at the Prototype International Data Center, *Pure appl. geophys.*, 159, 865-888.
- Hand, D.J. (1981), *Discrimination and Classification*, Wiley, New York, 218pp.
- Koch, K. and J. Schlittenhardt (2002), The use of teleseismic P-wave complexity for seismic event screening – Results determined from GRF and GERESS array data, *J. Seism.*, 6, 183-197.
- Ortiz, A.M., S.R. Taylor, T.J. Fitzgerald, and T. Wallace (2002), Rediscovering Signal Complexity Discriminants: A preliminary study for application to Regional Seismic and Radio Frequency Signatures, *Los Alamos National Laboratory, Los Alamos, NM*, LA-UR-02-7657.
- Stevens, J.L. and J.R. Murphy, Yield estimation from surface-wave amplitudes, *Pure. Appl. Geophys.*, 158, 2227-2251, 2001.
- Taylor, S.R., and P.D. Marshall (1991), Spectral discrimination between Soviet explosions and earthquakes using UK array data, *Geophys. J. Int.*, 106, 265 - 273.
- Taylor, S.R. (1996), Analysis of high-frequency Pg/Lg ratios from NTS explosions and western U.S. earthquakes, *Bull. Seism. Soc. Am.*, 86, 1042-1053.
- Wallace, T., D. Helmberger, and G. Engen (1983), Evidence of tectonic release from underground nuclear explosions in long-period P waves, *Bull. Seism. Soc. Am.*, 73, 593-613.
- Wallace, T. (1991), Body wave observations of tectonic release, in *Explosion Source Phenomenology*, AGU Monograph 65, Taylor, S.R., H.J. Patton , and P.G. Richards, eds., 161-170.
- Wiechert, D.H. (1971), Short period spectral discriminant for earthquake and explosion differentiation, *Z. Geophys.* 37, 147-152.

Figures

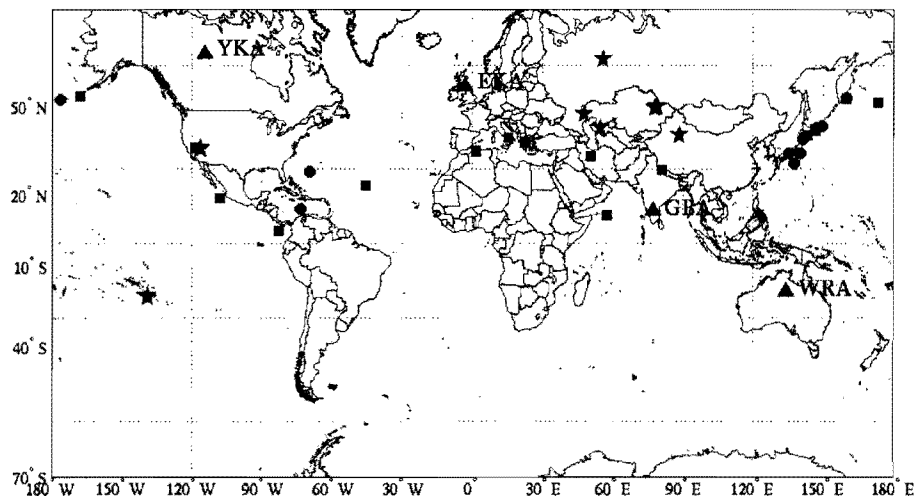


Figure 1. Map showing UK array stations and events. Stars are nuclear explosions, squares are shallow earthquakes (depth < 50 km) and circles are deep earthquakes (depth > 50 km).

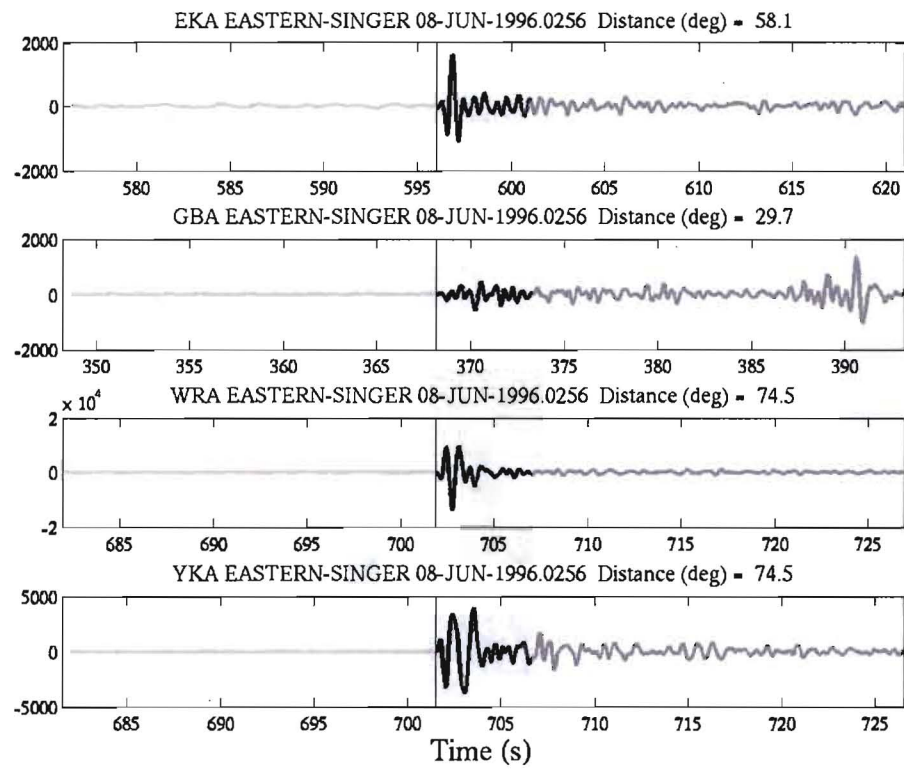


Figure 2. Example of Lop Nor nuclear explosion beams recorded at the four UK array stations. Light gray line indicates noise window, black line indicates signal window and medium gray line indicates coda window.

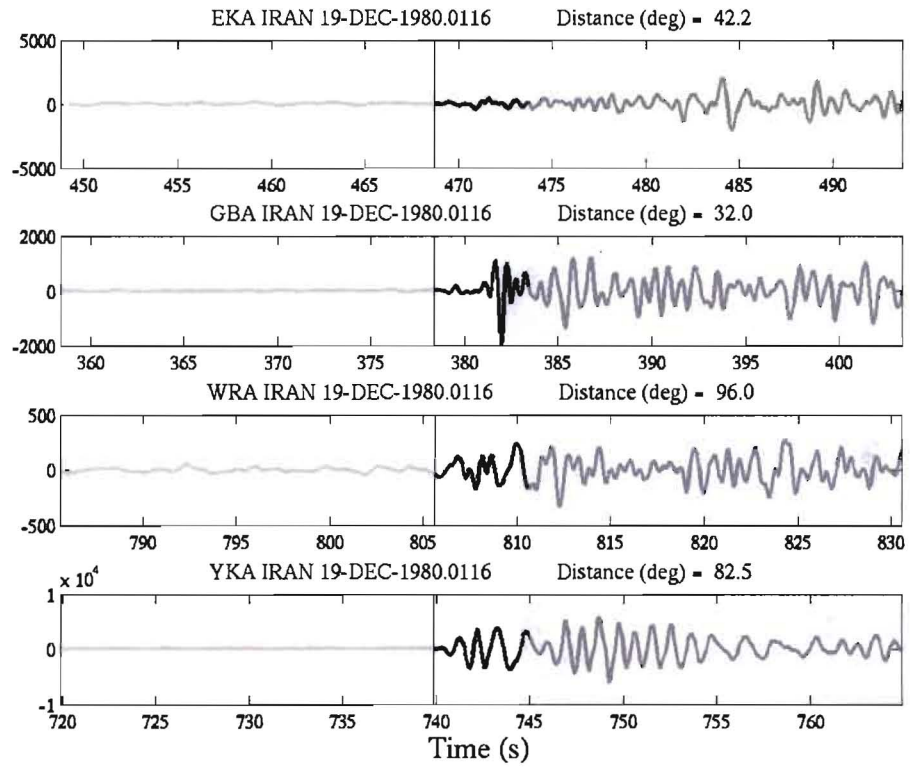


Figure 3. Example of shallow earthquake (depth = 29 km) beams recorded at the four UK array stations. Light gray line indicates noise window, black line indicates signal window and medium gray line indicates coda window.

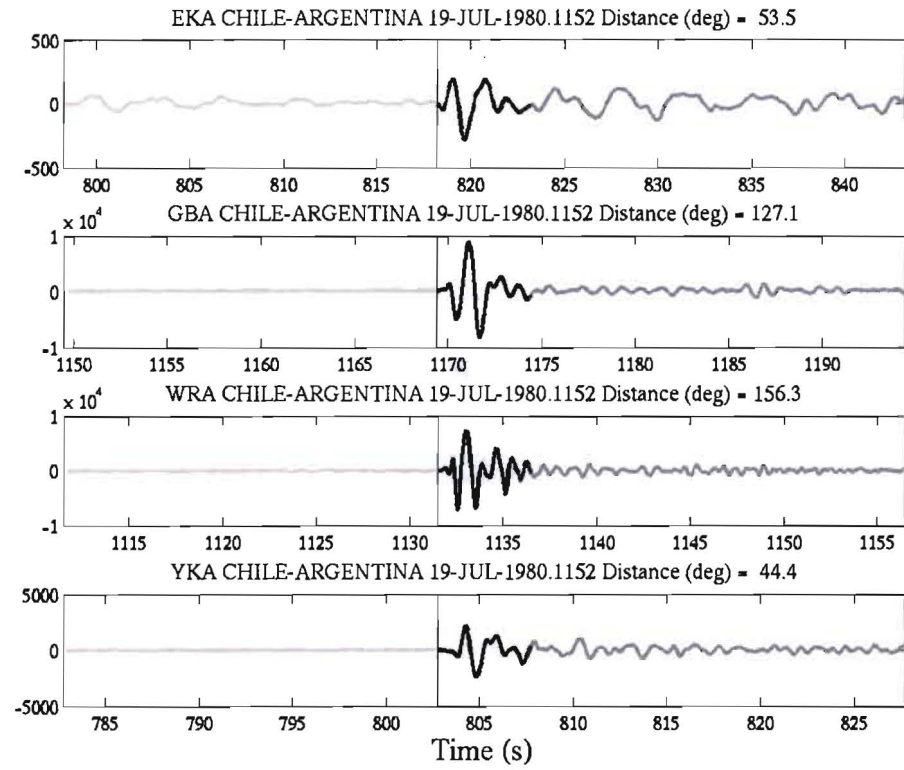


Figure 4. Example of deep earthquake beams (depth = 97 km) recorded at the four UK array stations. Light gray line indicates noise window, black line indicates signal window and medium gray line indicates coda window.

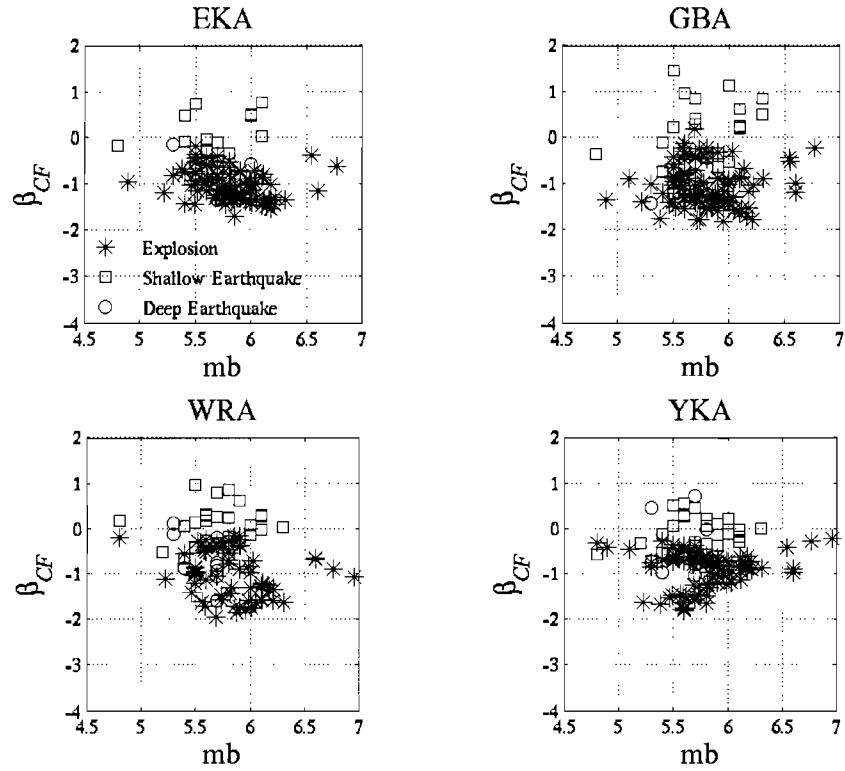


Figure 5. Complexity (β_{CF}) at the four UK array stations as a function of m_b . Asterisks are nuclear explosions, squares are shallow earthquakes (depth < 50 km) and circles are deep earthquakes (depth > 50 km). Number of measurements for each station in order of explosions, shallow earthquakes, deep earthquakes: EKA: 92, 16, 7; GBA: 95, 22, 6; WRA: 70, 27, 11; YKA: 94, 25, 8.

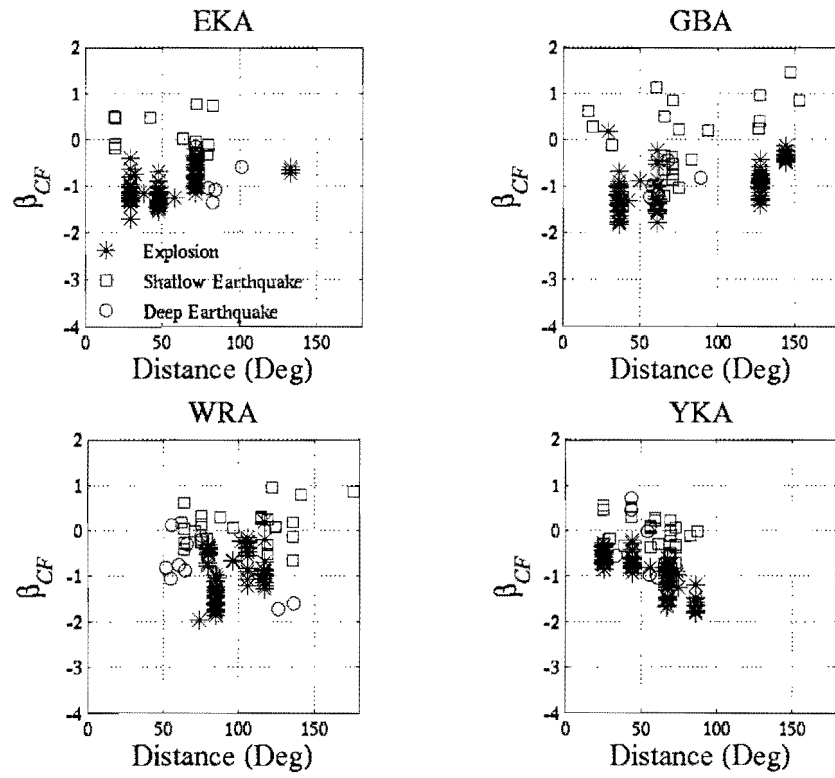


Figure 6. Complexity (β_{CF}) at the four UK array stations as a function of distance. Asterisks are nuclear explosions, squares are shallow earthquakes (depth < 50 km) and circles are deep earthquakes (depth > 50 km).

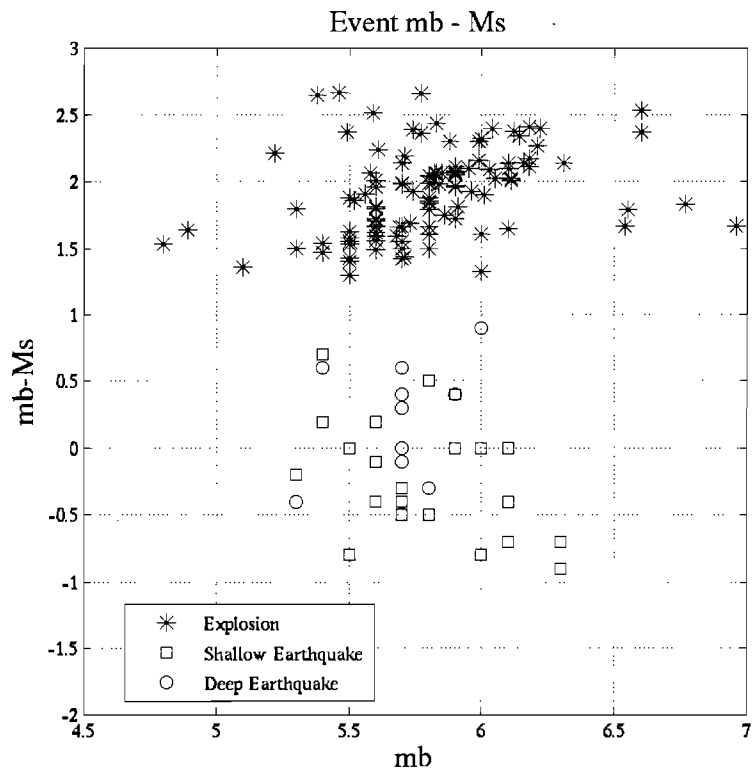


Figure 7. $m_b - M_s$ versus m_b for events from the ISC catalog and from Stevens and Murphy (2001). Asterisks are nuclear explosions, squares are shallow earthquakes (depth < 50 km) and circles are deep earthquakes (depth > 50 km). There are 92 explosions, 16 shallow earthquakes and 6 deep earthquakes in the figure.

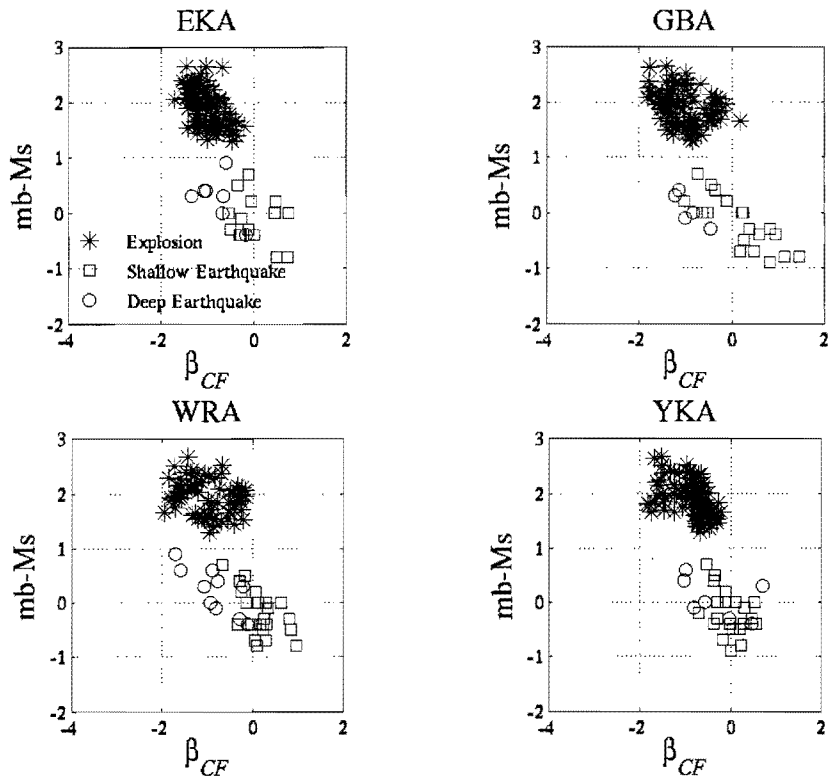


Figure 8. $m_b - M_s$ versus complexity (β_{CF}) at the four UK array stations. Asterisks are nuclear explosions, squares are shallow earthquakes (depth < 50 km) and circles are deep earthquakes (depth > 50 km).

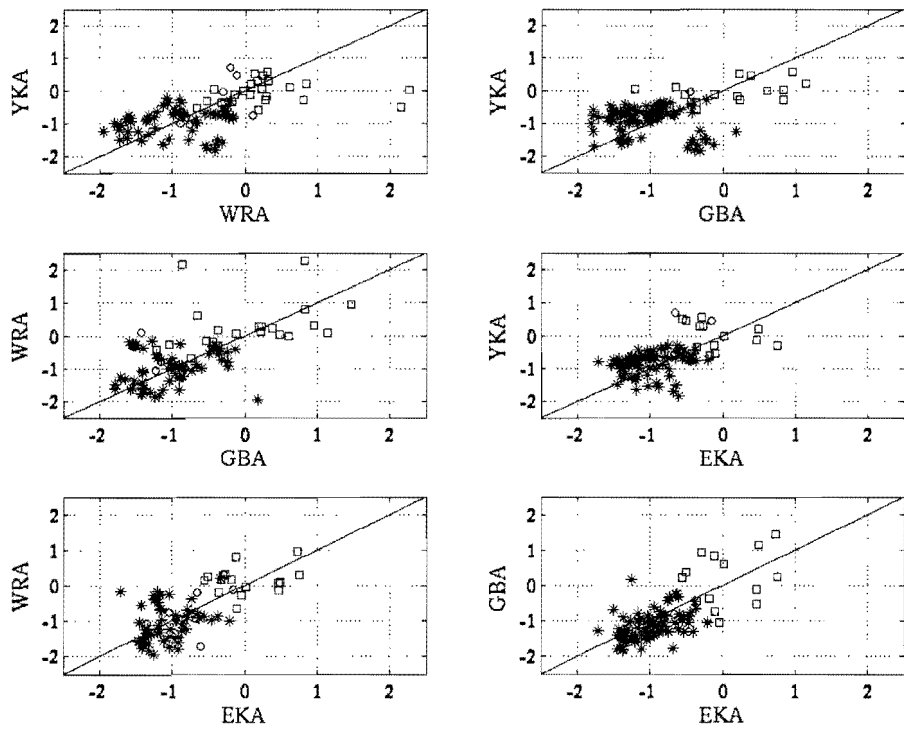


Figure 9. Bivariate plots for each combination of UK array stations. Asterisks are nuclear explosions, squares are shallow earthquakes (depth < 50 km). Black line is one-to-one.

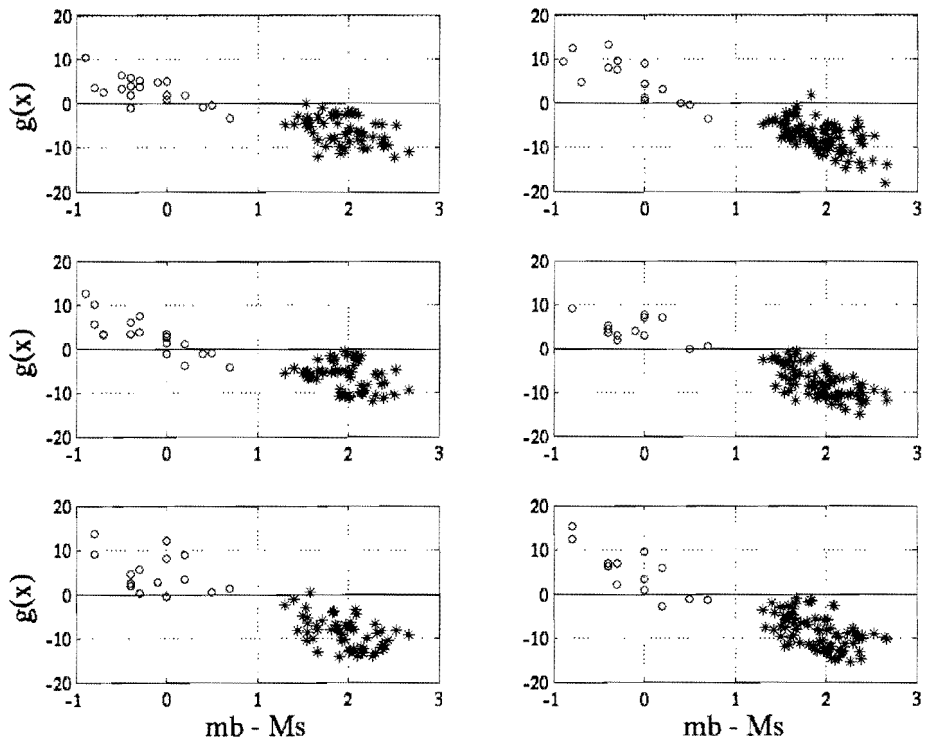


Figure 10. Discrimination function (Equation 2) for each UK array pair for shallow earthquakes (squares) and nuclear explosions (asterisks) plotted versus $m_b - M_s$.